This article has been accepted for inclusion in a future issue of this journal. Content is final as presented, with the exception of pagination.

On the Accuracy of the Cox–Strack Equation and Method for Contact Resistivity Determination

Milou van Rijnbach, Raymond J. E. Hueting, *Senior Member, IEEE*, Maciej Stodolny, Gaby Janssen, Jimmy Melskens, and Jurriaan Schmitz, *Senior Member, IEEE*

***Abstract*—The Cox–Strack method is commonly applied to assess the contact resistivity between a metal and a semiconductor since the 1960s, while the underlying assumptions have not yet been rigorously assessed. In this article, a combination of finite-element modeling and mathematical analysis is used to investigate the accuracy of the conventional Cox–Strack equation for generic metal–semiconductor junctions. A systematic error in the spreading resistance equation is quantified, and alternative, more accurate equations are presented. Furthermore, it is shown that commonly used experimental configurations can lead to highly overestimated contact resistivities. Guidelines are formulated for accurate extraction of the contact resistivity from the Cox–Strack measurements.**

***Index Terms*—Accuracy, contact resistivity, metal–semiconductor junctions, photovoltaics, resistance, test structures.**

I. Introduction

SEMICONDUCTOR devices rely on high-quality contacts between external, metallic leads and the semiconductor. As the device performance may be limited by these contacts, the resistance occurring at the interface between metal and semiconductor must be low and well-controlled in a fabrication process. This interface resistivity (contact resistivity) is, however, difficult to quantify precisely, as any measurement suffers from series resistance and current spreading effects [1]. This is particularly problematic when the contact resistivity is very low, as we find in contemporary silicon-integrated circuit technology (using advanced silicides) [2]. Accuracy issues are also reported in contemporary photovoltaic cells (see [3]).

Manuscript received January 8, 2020; revised February 12, 2020; accepted February 13, 2020. This work was supported by the Topconsortia for Knowledge and Innovation Solar Energy program of the Ministry of Economic Affairs of The Netherlands through the projects MIRACLE under Grant TEUE116139 and BRIGHT under Grant 1721101. The work of Jimmy Melskens was supported by the Netherlands Organisation for Scientific Research under the Dutch TTW-VENI Grant 15896. The review of this article was arranged by Editor E. A. Gutiérrez-D. *(Corresponding author: Jurriaan Schmitz.)*

Milou van Rijnbach, Raymond J. E. Hueting, and Jurriaan Schmitz are with the MESA+ Institute for Nanotechnology, University of Twente, 7500 AE Enschede, The Netherlands (e-mail: j.schmitz@utwente.nl).

Maciej Stodolny and Gaby Janssen are with TNO, Unit Energy Transition, 1755 LE Petten, The Netherlands.

Jimmy Melskens is with the Department of Applied Physics, Eindhoven University of Technology, 5600 MB Eindhoven, The Netherlands.

Color versions of one or more of the figures in this article are available online at http://ieeexplore.ieee.org.

Digital Object Identifier 10.1109/TED.2020.2974194

Two commonly used methods to quantify the contact resistivity between metal and semiconductor are the transfer length method (TLM, sometimes called transmission line method) [4] and the Cox–Strack method [5]. The latter was proposed in 1967 and is often used for compound semiconductor technologies [6]–[8] and photovoltaic cells [9]–[12].

Cox and Strack already reported an inaccuracy in their spreading resistance equation amounting to 8% at most, and later works indicated even larger inaccuracies with that equation [13], [14]. It is, therefore, important to account for this.

In this article, we show that the Cox–Strack equation is insufficiently exact to rely on without due consideration. Finite-element simulations are used to show where the problems occur and what causes them. The spreading resistance equations as presented in the literature are compared to such simulations (see Section IV), and a new function is proposed for the spreading resistance. Moreover, the assumption that the current path can be described as three resistors in series is investigated in this article (see Section V). In Section VI, we discuss the quantitative impact of the treated inaccuracies on the extracted contact resistivity. Using those findings, we formulate general guidelines to obtain accurate contact resistivity values with the Cox–Strack method.

II. Methods

The finite-element simulations in this article are conducted using the ATLAS-Silvaco software [15]. Axial symmetry is chosen combined with cylindrical coordinates. At the outer (noncontact) edges of the device, the homogeneous (reflecting) Neumann boundary conditions are imposed. The width of the simulated structure is always chosen much larger than the substrate thickness. Metal contacts are chosen neutral [16] and ohmic; the substrate doping is uniform. Dimensions, doping levels, and contact resistivities are then varied. We use parameters typical for crystalline silicon photovoltaic cells. The drift-diffusion equations are solved using Klaassen's mobility model [17]–[19]. The resulting current–voltage relations are checked for ohmic behavior.

III. Cox–Strack Method

Cox and Strack proposed to use a series of circular metal contacts on the semiconductor, with a range of diameters (see Fig. 1). The current is then measured at a given applied

This work is licensed under a Creative Commons Attribution 4.0 License. For more information, see http://creativecommons.org/licenses/by/4.0/

This article has been accepted for inclusion in a future issue of this journal. Content is final as presented, with the exception of pagination.

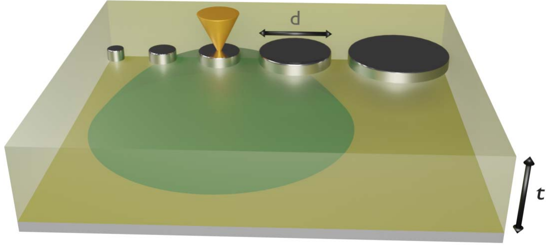

Fig. 1. Sketch of the measurement approach proposed by Cox and Strack [5]. Current flows from a probe needle (orange) via a circular ohmic contact with diameter d and through a semiconductor with thickness t into a bottom contact connecting the entire semiconductor slab. The conical shaped region (green) indicates the current spreading from a probed contact. The resistance of this stack is measured for several top contact diameters. Contact resistivity is then extracted using (4).

voltage from the circular contact through the substrate to its grounded metallized backside. They assumed that the total resistance measured R_T is the sum of three contributions: contact resistance R_c (between metal and semiconductor); spreading resistance R_s (in the semiconductor); and residual resistance R_0 ("due to the substrate or the backside contact")

$$R_\mathrm{T} = R_\mathrm{s} + R_\mathrm{c} + R_0. \quad (1)$$

In this article, we will refer to this assumption as the "three-resistor approximation." This series connection of resistors uses the implicit assumption that no potential variation may occur laterally at the nodes between the resistors. In other words, the potential in the semiconductor just under the metal contact and the potential just above the backside metallization should be independent of the lateral position.

Cox and Strack continued to describe the spreading resistance in the substrate with the following expression:

$$R_\mathrm{s} = \frac{\rho_\mathrm{w}}{2d} B \quad (2)$$

where ρ_w is the substrate resistivity, d is the diameter of the top contact, and B is a geometrical factor. Through electrolytic tank measurements, discussed in more detail in Section IV, Cox and Strack found that B depends on the ratio between the substrate thickness t and the top contact diameter d approximately according to

$$B \approx \frac{2}{\pi} \arctan\left(\frac{4t}{d}\right) \quad (3)$$

where t is the substrate thickness.[1]

Furthermore, R_c in (1) is determined by the contact resistivity (or specific contact resistance) ρ_c divided by the contact area. An implicit assumption here is that the current flow through the contact is uniform. Finally, the residual resistance R_0 is presumed geometry and resistivity independent, leading to the Cox–Strack equation

$$R_\mathrm{T} \approx \frac{\rho_\mathrm{w}}{\pi d} \arctan\left(\frac{4t}{d}\right) + \frac{\rho_\mathrm{c}}{\frac{1}{4}\pi d^2} + R_0. \quad (4)$$

[1]To be exact, Cox and Strack made use of low-ohmic substrates with a thin high-ohmic epitaxially grown semiconducting layer of 0.9 mil (23 μm). The thickness t is that of the epitaxial layer. Later studies apply the Cox–Strack method on semiconductor material with uniform resistivity.

The Cox–Strack contact resistivity determination procedure consists of measuring R_T on a range of top contacts with different diameters d and determining ρ_c and ρ_w from the $R_\mathrm{T}(d)$ dependence.

IV. Spreading Resistance Term

To estimate the spreading resistance, Cox and Strack conducted electrolytic tank measurements. These results match reasonably well with the arctangent function (3) with a maximum difference of 8% around $d = 3t$. Gelmont and Shur [20] confirm that (3) leads to a considerable (but unquantified) error for intermediate d/t ratios compared with a rigorous numerical calculation. Denhoff [13] presents finite-element calculations showing that the arctangent function is 13% off at $d = 2t$. Kristiansson *et al.* [14] report a maximum error of 16.6% compared with an exact solution published by Leong *et al.* [21].

The arctangent approximation is less accurate than Cox and Strack originally established, the root cause being the inaccuracy of the electrolytic tank measurements. It is difficult to state with certainty what caused this inaccuracy. Reference [5] does not provide any detail on these experiments, and other publications by Cox and Strack or the acknowledged Dr. J. R. Biard do not provide a clue. It is, however, likely that a planar salt bath was built according to the original concept [22], [23]. Mathematical corrections may have been made to translate the planar model to an axially symmetric configuration (as reported, for example, in [24]). Although accuracies better than 1% have been achieved with electrolytic bath experiments, a difficult aspect is the arrangement of side electrodes to impose the boundary conditions, especially when the bath is small [25].

In Fig. 2, we reproduce the original data by Cox and Strack [26] and compare these to the polynomial model of Denhoff and our own finite-element simulations. Details of the polynomial model and how we used it can be found in Appendix A.

Fig. 2 confirms that Denhoff's model matches well with finite-element modeling results and we assume these are accurate. Fig. 2 further confirms that the arctangent approximation is inaccurate over a wide range. It exhibits a maximum error of 17% at $d = 3t$. The full range practically used in experimentation is affected by this systematic error.

Following a geometrical approximation commonly applied for vertical power transistors [28]–[30], we derived a new physics-based equation that matches Denhoff's polynomial model to within 1%. It assumes that the current flows in a cone of resistive material capped by the top contact. Compared with Denhoff's polynomials, it has the advantage that a single equation covers the entire range of dimensions; furthermore, it contains only one fit parameter. As documented in Appendix B, we find

$$B = \frac{4}{\pi}\left[\frac{d}{2t} + \frac{4}{\pi} + \left(1 - \frac{4}{\pi}\right)\arctan\left(\frac{2d}{3t}\right)\right]^{-1}. \quad (5)$$

Fig. 2 indicates that (5) tightly follows Denhoff's polynomial equations. To visualize this more clearly, Fig. 3 shows the

This article has been accepted for inclusion in a future issue of this journal. Content is final as presented, with the exception of pagination.

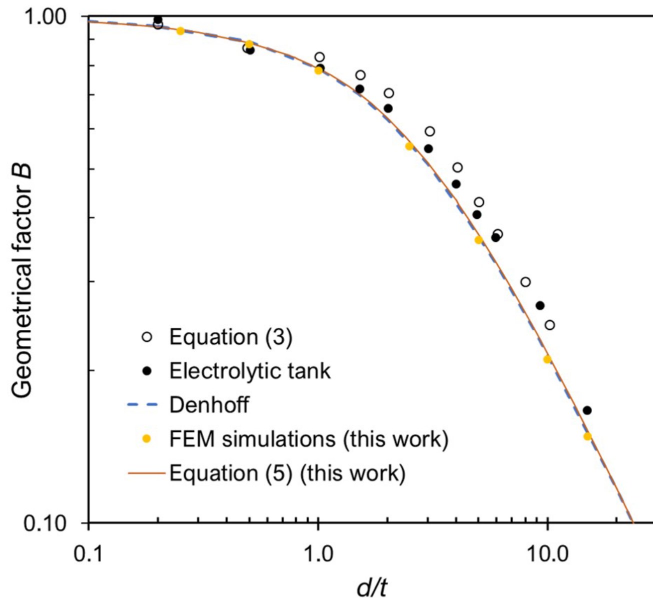

Fig. 2. Functional dependence of the geometrical parameter B on the ratio d/t according to the equations provided by Cox and Strack [5], Denhoff [13], finite-element simulations carried out with fixed t and varying d [27]; and (5). The electrolytic tank measurements as reported by Cox and Strack are also included [26].

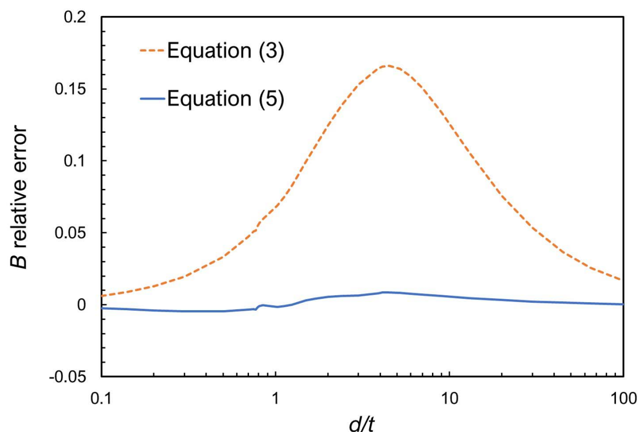

Fig. 3. Relative error on B of (3) and (5) compared with Denhoff's polynomials (see Appendixes A and B). The small kinks appearing around $d/t = 0.8$ and $d/t = 4$ indicate the switch to a different polynomial in Denhoff's formulation.

relative discrepancy between the approximating (3) and (5) on one hand and Denhoff's polynomials on the other hand.

Fig. 2 further allows us to derive a rule of thumb for the choice of contact diameters for the Cox–Strack method. To separate ρ_w from ρ_c, R_s should exhibit a functional dependence on d different from inverse quadratic because R_c has such a dependence [see (4)]. The parameter B should then not be inversely proportional to d/t. This occurs when d is smaller than $2t$. Test structures must, therefore, include diameters $d \approx 2t$ or smaller to accurately separate ρ_c.

V. Three-Resistor Equivalent Circuit

At first sight, there seems little question about the validity of the last two terms in the Cox–Strack equation [see (4)].

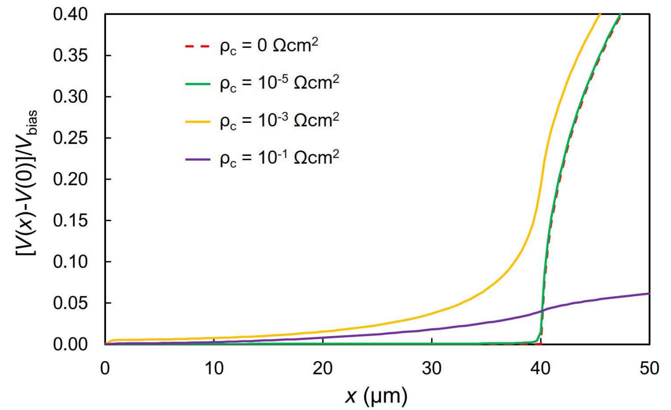

Fig. 4. Potential directly under the contact as a function of the lateral position x, where $x = 0$ indicates the center of the contact. The potential is related to the center potential $V(x = 0)$ and normalized to the externally applied test voltage V_{bias}. The contact diameter $d = 80$ μm, wafer resistivity $\rho_w = 3$ Ωcm, and wafer thickness $t = 165$ μm. The top contact was grounded, while a positive bias voltage was applied to the bottom electrode.

The total contact resistance R_c scales with the reciprocal area; a series resistance R_0 may appear in the measurement setup. However, an underlying assumption, as mentioned in Section III, is that we can describe the configuration as a lumped element circuit of three resistors in series. One case in which this assumption loses validity is when the top-metal resistivity cannot be neglected [31]. A more general approximation of a two-dimensional resistive system would be a distributed network of resistors, just as finite-element models assume.

Fig. 4 shows the potential directly under the contact for several contact resistivity values as computed by finite-element simulation. The potential shows a dependence on the distance to the contact center. The assumption that R_c and R_s can be modeled as two resistors in series implies that one fixed potential can be identified with a single point in between these resistors. Fig. 4 shows that this is not the case. At the highest and lowest ρ_c, the effect is very small; it presents itself most clearly in the intermediate case of $\rho_c = 10^{-3}$ Ωcm^2. In effect, the existence of a resistivity-dependent lateral potential gradient makes R_c and R_s mutually dependent when we maintain this three-element model.

Along with the lateral voltage drop, a nonuniform current density emerges at the contact interface. This nonuniformity is the largest at low ρ_c. While the original expressions of Cox and Strack imply a constant lateral voltage, a uniform current density through the contact, and a large nonuniformity of current density in the substrate, such conditions only occur when $\rho_c = 0$. In all other situations, an interplay exists between the current spreading in the contact and in the substrate. It is worth noting that also in other prior works, a uniform current density was assumed [31].

In the two limiting cases, $\rho_c = 0$ and $\rho_w = 0$, the region directly under the contact is short-circuited to an equipotential plane (the top contact or the bottom contact, respectively). In realistic situations, the lateral potential drop is appreciable, and the current through the contact

This article has been accepted for inclusion in a future issue of this journal. Content is final as presented, with the exception of pagination.

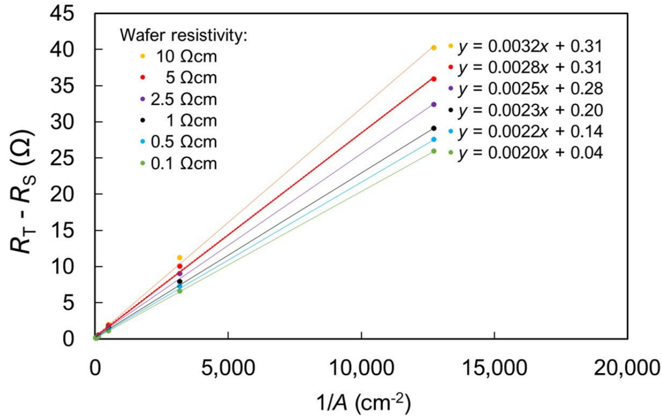

Fig. 5. Values of $R_T - R_s$ as determined using finite-element simulations (details: see main text). The slope of the curve, which should equal the input contact resistivity of 2 mΩcm^2, is systematically too high for wafer resistivities above 0.1 Ωcm. The series resistance R_0 appears dependent on the substrate resistivity from this analysis.

is nonuniform. Bearing notice of the different dimensionality of ρ_c and ρ_w, the ratio between ρ_c and $\rho_w t$ determines the ratio R_c:R_s, the significance of the lateral variation of potential and current density at the contact, and their effect on the contact resistivity as quantified by the Cox–Strack method.

Simulation of an elementary construction, as shown in Fig. 1, illustrates how the three-resistor approximation can lead to significant errors. The simulated configuration has an n-type monocrystalline silicon substrate with $t = 200$ μm and 5 Ωcm resistivity. We first determine the spreading resistance R_s by simulation for a range of diameters by setting ρ_c to an insignificantly low value for the front contact and the back contact. Consequently, $R_T = R_s$. Then, the total resistance R_T is determined with a realistic top contact resistivity of 2 mΩcm^2. The chosen values are representative of contemporary silicon solar cells.

The Cox–Strack equation (4) can be written as

$$R_T - R_s = \frac{\rho_c}{\frac{1}{4}\pi d^2} + R_0 = \frac{\rho_c}{A} + R_0 \qquad (6)$$

in which $A = \frac{1}{4}\pi d^2$ the top contact area. A linear fit of $R_T - R_s$ versus $1/A$ yields estimates for ρ_c and R_0.

Fig. 5 shows the outcome of this exercise. The fits have a good $R^2 > 0.999$ but deliver erroneous values. The extracted contact resistivity strongly depends on the substrate doping level and is up to 60% too high. The fit error becomes negligible around 0.1-Ωcm substrate resistivity. At this point, $\rho_c/\rho_w t = 1$ and the errors emerge when $\rho_c/\rho_w t < 1$. Indeed, it was earlier observed that lower substrate resistivities yield more accurate contact resistivity values with the Cox–Strack method [6], [31].

A further observation from the same simulation exercise is that the obtained R_0 is nonzero, whereas no back contact resistance was assumed. Additional simulations indicate that R_0 as determined in this manner depends on ρ_w, ρ_c, and t [27]. Again, these are consequences of the erroneous three-resistor approximation of (6).

TABLE I
PARAMETER VALUES FOR THE FINITE-ELEMENT SIMULATIONS USED TO QUANTIFY THE PARAMETER EXTRACTION ERRORS WITH THE COX–STRACK METHOD

	t = 16.5 μm	t = 165 μm
$\rho_c(\Omega\text{cm}^2)$	10^{-6}, 10^{-5}, 10^{-4}, 10^{-3}, 10^{-2}	same values ×10
$\rho_w(\Omega\text{cm})$	0.5, 3, 10	same values
d (μm)	6, 8, 12, 20, 40, 100, 200	same values ×10

VI. IMPACT ON RESISTIVITY DETERMINATION

An accurate determination of contact resistivity requires good control over measurement circumstances. In general, the following aspects should be taken into account.

1) Measurement conditions should be chosen such that voltage and current are accurately determined. High injection effects and current-induced heating of the test structure should be negligible.
2) The diameters of the top contacts should be known to sufficient accuracy. Textured wafers (as common for solar cells) may lead to uncertainty in both the contact area and the wafer thickness.
3) The top and bottom metal contacts to a semiconducting wafer should be ohmic. Wang *et al.* [32] recently treated the effects of a Schottky barrier on the Cox–Strack method.

However, even if these effects are under control, the Cox–Strack method may yield erroneous ρ_c and ρ_w values because of the two inherent weaknesses in the method described in Sections IV and V. The used model can lead to inaccurate estimates of R_c and R_s for each probed diameter d. The effect of these errors on the extracted ρ_c and ρ_w is further quantified below.

A wide range of finite-element simulations was conducted, in which the parameters d, ρ_c, ρ_w, and t were varied, as listed in Table I. For each set of (ρ_c, ρ_w, t), the $R_T(d)$ data were used to obtain ${\rho_c}^{fit}$ and ${\rho_w}^{fit}$ in a nonlinear least-squares fit procedure. The fit function was the three-resistor approximation using either the arctangent approximation (3), Denhoff's polynomials, or (5) to estimate the B-parameter in the spreading resistance.

These fits gave good agreement for all $R_T(d)$ data. Using the Denhoff polynomials, the difference between fit and simulated R_T data points was typically $< 1\%$ with incidental maximum variations of 5%. Using the Cox–Strack equations, incidental deviations up to 8% were found.

The fit values ${\rho_c}^{fit}$ and ${\rho_w}^{fit}$ can then be directly compared with the input values ${\rho_c}^{input}$ and ${\rho_w}^{input}$ in the simulation. We define the (relative) error as

$$\text{Error in fitted } \rho_c = \frac{\Delta\rho_c}{\rho_c} = \frac{\rho_c^{fit} - \rho_c^{input}}{\rho_c^{input}}; \qquad (7)$$

and likewise for ρ_w.

Figs. 6 and 7 show the results. For clarity, data are only shown for $t = 16.5$ μm, but essentially identical results were obtained for $t = 165$ μm. Data are plotted as a function of

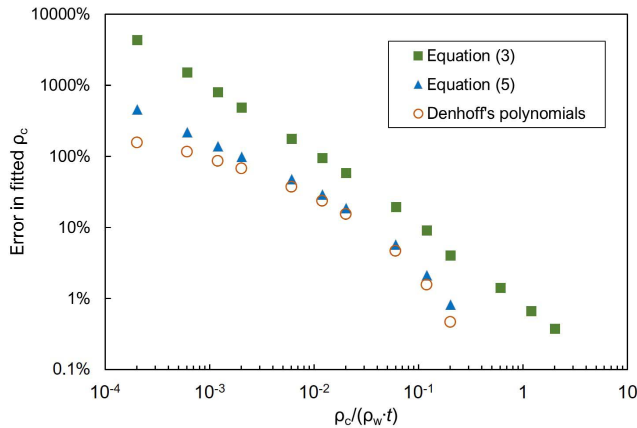

Fig. 6. Systematic error on ρ_c extracted using the Cox–Strack method when using (3), Denhoff's polynomials, or (5) to calculate R_s.

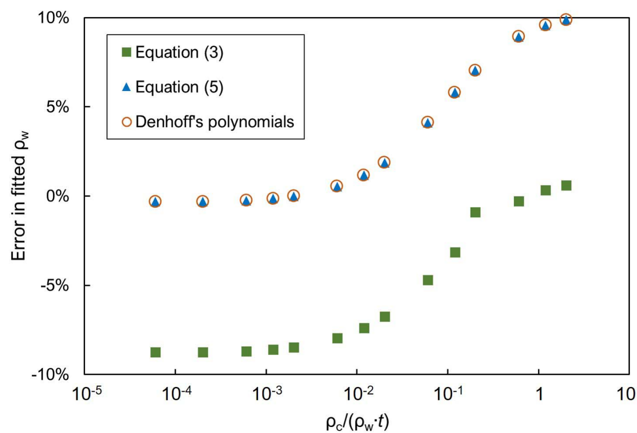

Fig. 7. Systematic error on ρ_w extracted using the Cox–Strack method when using (3), Denhoff's polynomials, or (5) to calculate R_s.

$\rho_c/\rho_w t$ as motivated in Section V. From the lack of scatter in the data set, it is clear that the error introduced by the model imperfections is solely determined by the $\rho_c/\rho_w t$ ratio. We find that it is necessary to fit ρ_w (even if this is known) in order to obtain an accurate value for ρ_c. A comparison of Figs. 5 and 6 corroborates this.

Fitting the ρ_w value gives superior agreement with the simulation data because the expressions for the spreading resistance are only strictly valid when ρ_c is zero. When ρ_c increases, the current density distribution at the contact becomes more and more uniform, leading to a larger contribution of the spreading resistance, i.e., an apparently larger ρ_w.

Regardless of the expression used for the spreading resistance, the Cox–Strack method considerably overestimates ρ_c at low contact resistivity, which is, in general, the area of interest. The error in ρ_w, however, is quite acceptable across the entire range. In order to keep the ρ_c accuracy better than 10%, the $\rho_c/\rho_w t$ ratio should be above 0.12 if (3) is used. This requirement can be relaxed to $\rho_c/\rho_w t > 0.03$ when using the Denhoff polynomials or (5).

Extracted values could also be corrected manually on the basis of the trend shown in Figs. 6 and 7. The systematic error on ρ_c roughly amounts to

$$\frac{\Delta\rho_c}{\rho_c} \approx 1.2\% \frac{\rho_w t}{\rho_c} \tag{8}$$

when the conventional Cox–Strack equation is used.

Fig. 6 shows that the applicability of the Cox–Strack method is questionable at lower ratios $\rho_c/\rho_w t$. Given the accuracy of the finite-element calculations, there is no appreciable difference between the accuracy of (5) and Denhoff's polynomials.

As a final note, the experimental measurement accuracy was not considered in Figs. 6 and 7; they only quantify the fundamental systematic error of the Cox–Strack extraction approach. Any measurement inaccuracy will show a similar trend with $\rho_c/\rho_w t$ because the inaccuracy goes mostly to R_s or R_c, whichever is the smallest.

VII. Conclusion

In this article, the accuracy of the Cox–Strack method [5] is analyzed and quantified. It is found that the formalism accompanying it has two deficiencies.

The first source of inaccuracy is the spreading resistance equation as proposed by Cox and Strack, which produces a systematic error up to 17% as quantified in Fig. 3. Polynomial approximations reach much better accuracies, as does the modified conical approximation proposed in this article [see (5)]. The analysis of the spreading resistance further yields the design criterion that diameters $d < 2t$ should be used to obtain useful data for contact resistivity determination.

This article shows how lateral potential gradients may exist directly under the contact and nonuniform current densities occur in the contact. This renders the three-resistor equivalent circuit incorrect, leading to errors in the extraction of contact resistivity. It is argued that the three-resistor equivalent circuit is safely applied when the fraction $\rho_c/\rho_w t$ is not too low; otherwise, the error in the extracted contact resistivity can be very significant. In the latter case, data are the best compared with finite-element simulations for a more precise contact resistivity estimate.

As the errors reported in this article are systematic, an alternative approach is to determine the contact resistivity with the inaccurate extraction method and manually correct for the error using Fig. 6 or (8).

This article provides tangible guidelines for an accurate determination of ρ_c using the Cox–Strack methodology that can be applied in a wide range of semiconductor technologies, including photovoltaic cells, compound semiconductor devices, and silicon integrated circuits.

Appendix A
Denhoff's Polynomials

Denhoff used mathematical approximations and polynomial fits to finite-element simulation results in order to establish equations for $B(d/t)$. Denhoff first defined the aspect ratio h as

$$h = \frac{2t}{d}. \tag{9}$$

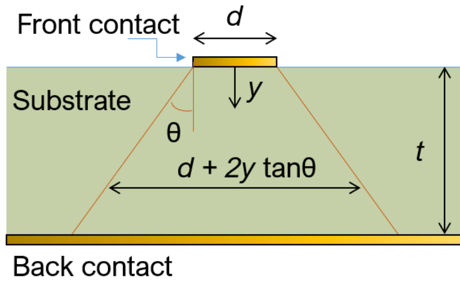

Fig. 8. Geometry of the model assuming the current spreads out linearly with depth y with a tapering angle θ from a front contact with diameter d.

For $h > 1$, Denhoff then determined the spreading resistance as a power series of h. Expressed in terms of B, this is

$$B = \left[1 + 0.441271\frac{1}{h} + 0.194720\frac{1}{h^2} - 0.009732\frac{1}{h^3} - 0.046505\frac{1}{h^4} + 0.002110\frac{1}{h^5} + 0.052204\frac{1}{h^6} - 0.011044\frac{1}{h^7}\right]^{-1}. \quad (10)$$

For small h, Denhoff fitted a fifth-order polynomial to finite-element simulation results. The result for $0 < h < 2.6$ is

$$B = 4[0.31338h - 0.25134h^2 + 0.12512h^3 - 0.03436h^4 + 0.003908h^5]. \quad (11)$$

For $0 < h < 0.5$, a similar fit approach yields

$$B = 4[0.31844h - 0.28374h^2 + 0.21145h^3 - 0.17193h^4 + 0.10657h^5]. \quad (12)$$

In this article, we used (10) for $h > 2.6$, (11) for $0.5 < h < 2.6$, and (12) for $0 < h < 0.5$.

Appendix B
Conical Approximation

The spreading resistance in the substrate is commonly approximated as a triangular conduction path in the area of (vertical) power transistors [28]–[30]. For circular contacts, one can analogously assume a conical shape for the current conducting region under the contact.

Fig. 8 shows the configuration under study. If we assume that the current spreads out under an angle θ, a wider path is used for conduction as we get deeper into the wafer.

The resistance contribution of an infinitesimal slab with thickness dy at depth y then amounts to

$$dR_s = \frac{\rho_w}{\frac{1}{4}\pi(d + \alpha y)^2}dy \quad (13)$$

where $\alpha = 2\tan(\theta)$. Integration over y yields

$$R_s = \frac{4}{\pi}\frac{\rho_w t}{d(d + \alpha t)}. \quad (14)$$

The equation represents a parallel connection of two resistors, one cylindrical under the contact (R_{cyl}), and one describing the edge (R_{edge}):

$$R_{cyl} = \frac{\rho_w t}{\frac{1}{4}\pi d^2}; \quad R_{edge} = \frac{4\rho_w}{\alpha\pi d}. \quad (15)$$

The expression for B in this conical approximation becomes

$$B = \frac{8t}{\pi(d + \alpha t)} = \frac{4}{\pi}\frac{2t}{d}\left(\frac{\alpha t}{d} + 1\right)^{-1}. \quad (16)$$

This equation accurately estimates B for $\frac{2t}{d} < 1$ when we use $\theta = 45^\circ$ (so $\alpha = 2$) after [30]. However, in the limit $d/t \to 0$, the function B should converge to 1, yielding $\alpha = \frac{8}{\pi}$. The underlying problem is that θ becomes larger than 45° when d goes to zero. If we introduce a slight d/t dependence in α, this problem is fixed. We propose the following correction:

$$B = \frac{4}{\pi}\left[\frac{d}{2t} + \frac{4}{\pi} + \left(1 - \frac{4}{\pi}\right)\arctan\left(\frac{2d}{3t}\right)\right]^{-1}. \quad (17)$$

This function meets the Denhoff polynomials with less than 1% relative error over the full range of d/t. The average relative difference amounts to only 0.4%. Its merit is that a single function can be used for all d/t ratios. The factor 2/3 in the arctangent is the only fit parameter in this equation, established through a minimization of the error between this function and Denhoff's polynomials.

Acknowledgment

The authors would like to thank B. Macco of the Eindhoven University of Technology for his contributions to the artwork.

References

[1] S. S. Cohen, "Contact resistance and methods for its determination," *Thin Solid Films*, vol. 104, nos. 3–4, pp. 361–379, 1983, doi: 10.1016/0040-6090(83)90577-1.
[2] N. Stavitski, M. J. H. van Dal, A. Lauwers, C. Vrancken, A. Y. Kovalgin, and R. A. M. Wolters, "Evaluation of transmission line model structures for silicide-to-silicon specific contact resistance extraction," *IEEE Trans. Electron Devices*, vol. 55, no. 5, pp. 1170–1176, May 2008, doi: 10.1109/TED.2008.918658.
[3] K. C. Fong *et al.*, "Optimization and characterization of phosphorus diffused LPCVD polysilicon passivated contacts with low pressure tunnel oxide," in *Proc. IEEE 7th World Conf. Photovoltaic Energy Convers. (WCPEC)*, Jun. 2018, pp. 2002–2005, doi: 10.1109/PVSC.2018.8547448.
[4] D. K. Schroder, *Semiconductor Material and Device Characterization*, 3rd ed. Hoboken, NJ, USA: Wiley, 2015.
[5] R. H. Cox and H. Strack, "Ohmic contacts for GaAs devices," *Solid State Electron.*, vol. 10, no. 12, pp. 1213–1218, 1967.
[6] R. P. Gupta, J. B. White, O. D. Iyore, U. Chakrabarti, H. N. Alshareef, and B. E. Gnade, "Determination of contact resistivity by the Cox and Strack method for metal contacts to bulk bismuth antimony telluride," *Electrochem. Solid-State Lett.*, vol. 12, no. 8, pp. H302–H304, 2009, doi: 10.1149/1.3143918.
[7] P. A. Sharma *et al.*, "Electrical contact uniformity and surface oxidation of ternary chalcogenide alloys," *AIP Adv.*, vol. 9, no. 1, Jan. 2019, Art. no. 015125, doi: 10.1063/1.5081818.
[8] C.-H. Lin *et al.*, "Single-crystal-Ga_2O_3/polycrystalline-SiC bonded substrate with low thermal and electrical resistances at the heterointerface," *Appl. Phys. Lett.*, vol. 114, no. 3, Jan. 2019, Art. no. 032103, doi: 10.1063/1.5051720.
[9] X. Yang, Q. Bi, H. Ali, K. Davis, W. V. Schoenfeld, and K. Weber, "High-performance TiO_2-based electron-selective contacts for crystalline silicon solar cells," *Adv. Mater.*, vol. 28, no. 28, pp. 5891–5897, May 2016, doi: 10.1002/adma.201600926.
[10] J. Bullock *et al.*, "Survey of dopant-free carrier-selective contacts for silicon solar cells," in *Proc. 43rd IEEE PVSC Conf.*, 2016, pp. 210–214, doi: 10.1109/PVSC.2016.7749580.
[11] Y. Wan *et al.*, "Conductive and stable magnesium oxide electron-selective contacts for efficient silicon solar cells," *Adv. Energy Mater.*, vol. 7, no. 5, Nov. 2016, Art. no. 1601863, doi: 10.1002/aenm.201601863.

[12] B. Macco *et al.*, "Atomic-layer deposited Nb_2O_5 as transparent passivating electron contact for c-Si solar cells," *Sol. Energy Mater. Sol. Cells*, vol. 184, pp. 98–104, Sep. 2018, doi: 10.1016/j.solmat.2018.04.037.

[13] M. W. Denhoff, "An accurate calculation of spreading resistance," *J. Phys. D, Appl. Phys.*, vol. 39, no. 9, pp. 1761–1765, Apr. 2006, doi: 10.1088/0022-3727/39/9/009.

[14] S. Kristiansson, F. Ingvarson, and K. O. Jeppson, "Compact spreading resistance model for rectangular contacts on uniform and epitaxial substrates," *IEEE Trans. Electron Devices*, vol. 54, no. 9, pp. 2531–2536, Sep. 2007, doi: 10.1109/TED.2007.902689.

[15] *Atlas Device Simulation Software, Version 5.25.2.C*, Silvaco, Santa Clara, CA, USA, 2017.

[16] D. K. Schroder and D. L. Meier, "Solar cell contact resistance—A review," *IEEE Trans. Electron Devices*, vol. ED-31, no. 5, pp. 637–647, May 1984, doi: 10.1109/T-ED.1984.21583.

[17] D. B. M. Klaassen, "A unified mobility model for device simulation—I. Model equations and concentration dependence," *Solid State Electronics*, vol. 35, no. 7, pp. 953–959, 1992, doi: 10.1016/0038-1101(92)90325-7.

[18] D. B. M. Klaassen, "A unified mobility model for device simulation—II. Temperature dependence of carrier mobility and lifetime," *Solid State Electronics*, vol. 35, no. 7, pp. 961–967, 1992, doi: 10.1016/0038-1101(92)90326-8.

[19] M. N. Darwish, J. L. Lentz, M. R. Pinto, P. M. Zeitzoff, T. J. Krutsick, and H. Ha Vuong, "An improved electron and hole mobility model for general purpose device simulation," *IEEE Trans. Electron Devices*, vol. 44, no. 9, pp. 1529–1538, Sep. 1997, doi: 10.1109/16.622611.

[20] B. Gelmont and M. Shur, "Spreading resistance of a round ohmic contact," *Solid-State Electron.*, vol. 36, no. 2, pp. 143–146, 1993, doi: 10.1016/0038-1101(93)90132-A.

[21] M. S. Leong, S. C. Choo, and L. S. Tan, "The role of source boundary condition in spreading resistance calculations," *Solid-State Electron.*, vol. 21, no. 7, pp. 933–941, 1978, doi: 10.1016/0038-1101(78)90291-5.

[22] G. Kirchhoff, "Ueber den Durchgang eines elektrischen Stromes durch eine Ebene, insbesondere durch eine Kreisförmige," *Annalen der Physik und Chemie, Band LXIV*, vol. 64, no. 4, pp. 497–514, 1845.

[23] W. G. Adams, "Bakerian lecture—On the forms of equipotential curves and surfaces and lines of electric force," *Proc. Roy. Soc.*, vol. 23, p. 280, Jan. 1875.

[24] A. L. Samuel, "Some notes on the design of electron guns," *Proc. IRE*, vol. 33, no. 4, pp. 233–240, Apr. 1945, doi: 10.1109/JRPROC.1945.233874.

[25] W. W. Hansen and O. C. Lundstrom, "Experimental determination of impedance functions by the use of an electrolytic tank," *Proc. IRE*, vol. 33, no. 8, pp. 528–534, Aug. 1945, doi: 10.1109/JRPROC.1945.230510.

[26] *Graphgrabber Version 2.01*, Quintessa, Henley-on-Thames, U.K., 2020.

[27] M. van Rijnbach, "Accurate extraction of the specific contact resistance in polysilicon passivated solar cells," M.S. thesis, Dept. Elect. Eng., Univ. Twente, NB Enschede, The Netherlands, 2019.

[28] S. C. Sun and J. D. Plummer, "Modeling of the on-resistance of LDMOS, VDMOS, and VMOS power transistors," *IEEE Trans. Electron Devices*, vol. 27, no. 2, pp. 356–367, Feb. 1980, doi: 10.1109/T-ED.1980.19868.

[29] C. Hu, M.-H. Chi, and V. M. Patel, "Optimum design of power MOSFET's," *IEEE Trans. Electron Devices*, vol. ED-31, no. 12, pp. 1693–1700, Dec. 1984, doi: 10.1109/T-ED.1984.21773.

[30] B. J. Baliga, *Fundamentals of Power Semiconductor Devices*. New York, NY, USA: Springer 2008.

[31] M. Ahmad, T. Ganguli, S. Major, N. R. Ry, and B. M. Arora, "Variations in the Cox and Strack curve for non-zero metal resistance," *Solid-State Electronics*, vol. 42, no. 4, pp. 473–476, 1998, doi: 10.1016/S0038-1101(97)00200-1.

[32] W. Wang *et al.*, "An expanded cox and strack method for precise extraction of specific contact resistance of transition metal Oxide/n-silicon heterojunction," *IEEE J. Photovolt.*, vol. 9, no. 4, pp. 1113–1120, Jul. 2019, doi: 10.1109/JPHOTOV.2019.2917386.